Persistent current driven by the Josephson effect in a triple-quantum-dot ring with superconducting leads

Guangyu Yi, Zhichao Li, Xiaohui Chen, Haina Wu, and Wei-Jiang Gong*
College of Sciences, Northeastern University, Shenyang 110819, China
(Received 14 January 2013; revised manuscript received 13 May 2013; published 29 May 2013)

The Josephson effect in a superconductor/triple-quantum-dot ring/superconductor structure is theoretically investigated. We find that in this structure, interdot spin correlation can be driven, which contributes to the occurrence of new 0 and π phases of the Josephson current. Moreover, in the 0-π phase-transition process, an intermediate bistable phase appears in which the Josephson current is completely suppressed. By analyzing the interdot spin correlation, the electron motion mechanism is clarified. We then attribute the disappearance of the Josephson current to the occurrence of the Josephson-Fano effect. What is interesting is that the disappearing Josephson current is accompanied by the apparent persistent current in the ring whose direction is determined by the superconducting phase difference. With the calculated results, we consider such a structure to be a candidate for the realization of the persistent current bit.

DOI: 10.1103/PhysRevB.87.195442 PACS number(s): 73.63.Kv, 71.70.Ej, 72.25.−b

I. INTRODUCTION

In recent years, great advances in fabricating the hybrid nanostructures with quantum dots (QDs), molecules, and carbon nanotubes attached to conducting leads have attracted an increasing interest in quantum transport through such low-dimensional systems. The main reason is that in most of these systems, electron correlations, e.g., the Kondo effect, play a significant role in contributing to the quantum transport properties.[1–3] More interestingly, QDs have the advantage of coupling to one another to construct various-configuration QD molecules. In QD molecules, the intradot and interdot electron correlations induce abundant transport behaviors, such as the SU(N) Kondo effect[4] and Fano-Kondo effect.[5] On the other hand, the properties of leads influence the quantum transport through QD structure in a substantial way. Specifically, when the leads are superconductors, the interplay between the Josephson and electron correlation effects causes intricate 0-π phase-transition behaviors.[6–15] This prediction has been confirmed experimentally in both carbon nanotubes and semiconducting nanowires.[16,17] Motivated by this result, many groups dedicated themselves to the Josephson effect in the structure of QD molecules coupled to superconducting leads. It has been observed that the complicated electron correlations in QD molecule systems lead to some more intricate phase transition of the Josephson current.[18–20]

With respect to the QD molecules, the coupled triple-QD (TQD) structure is typical and has recently been paid much attention from both experimental and theoretical aspects.[21,22] One reason is the desire to develop capabilities to design increasingly complex quantum systems at both single-particle and many-particle levels. Such a quantum system by design might serve as a laboratory for correlated electron systems as well as a prototype quantum processor based on charge and/or spin in QDs.[23,24] The other applications of a TQD are in the area of quantum computation. The three-spin system is the smallest quantum system where quantum teleportation can be realized. The TQD system allows for the realization of the simplest three-level system and hence allows for the application of tools known from quantum optics, such as coherent electronic transfer using adiabatic passage or rectification.[25,26] On the other hand, a TQD allows one to study new phenomena not present in single or double QDs. For example, a TQD is the smallest artificial molecule where topology plays a role, as it can form either a linear or triangular molecule.[27–30] Particularly, three QDs can be coupled to one another and form the TQD ring (TQDR). Such a circular geometry allows for the interplay between quantum interference and electron-electron interactions, leading to various transport phenomena.[31] Furthermore, if a TQDR is coupled to three terminals, the spin-orbit interaction can drive the notable spin polarization, and even the pure spin current can be observed in the nonequilibrium case.[32]

It is natural to think that the abundant physics included in the TQD structure certainly plays a nontrivial role in modulating the Josephson effect. With such an idea, in this work we consider one typical structure, i.e., the TQDR, to couple to two superconducting leads, and investigate the interplay among the Josephson effect, quantum interference, and the electron correlations. As a consequence, we observe an interdot spin correlation which contributes to the new 0-π phase transition of the Josephson current. Additionally, in such a 0-π transition process, an intermediate bistable phase emerges in which the Josephson current is completely suppressed. Further investigation shows that the disappearance of the Josephson current is accompanied by the maximal persistent current in the ring. We consider such a structure to be a candidate for the realization of the persistent current bit.

II. THEORY

The Hamiltonian of the superconductor/triple-quantum-dot ring/superconductor (S/TQDR/S) structure is written as $H = \sum_\alpha H_\alpha + H_D + H_T$, where

$$H_\alpha = \sum_{k\sigma} \varepsilon_{\alpha k} a^\dagger_{\alpha k\sigma} a_{\alpha k\sigma} + \sum_k (\Delta e^{i\varphi_\alpha} a_{\alpha k\downarrow} a_{\alpha -k\uparrow} + \Delta e^{-i\varphi_\alpha} a^\dagger_{\alpha -k\uparrow} a^\dagger_{\alpha k\downarrow}),$$

$$H_D = \sum_{\sigma,j=1}^{3} \varepsilon_j d_{j\sigma}^{\dagger} d_{j\sigma} + \sum_{\sigma,j=1}^{3} (t_j d_{j+1\sigma}^{\dagger} d_{j\sigma} + \text{H.c.}) + \sum_j U_j n_{j\uparrow} n_{j\downarrow},$$
$$H_T = \sum_{k\sigma} (V_{Lk} a_{Lk\sigma}^{\dagger} d_{1\sigma} + V_{Rk} a_{Rk\sigma}^{\dagger} d_{2\sigma} + \text{H.c.}). \quad (1)$$

H_α ($\alpha = L, R$) is the standard BCS mean-field Hamiltonian for the superconducting leads with phase φ_α and energy gap Δ. H_D models the TQDR, and H_T denotes the tunneling between lead-$L(R)$ and QD-1(2). $a_{\alpha k\sigma}^{\dagger}$ and $d_{j\sigma}^{\dagger}$ ($a_{\alpha k\sigma}$ and $d_{j\sigma}$) are operators to create (annihilate) an electron with momentum k and spin orientation σ in the lead-σ and in QD-j, respectively. $\varepsilon_{\alpha k}$ and ε_j denote the corresponding energy levels. U_j indicates the strength of intradot Coulomb repulsion, and t_j is the interdot coupling coefficient. $V_{\alpha k}$ denotes the coupling between lead-α and the QDs.

In such a structure, the Josephson current at zero temperature can be evaluated by deriving the ground-state energy $E_{\min}$ with respect to the superconducting phase difference, i.e.,

$$I_J = \frac{2e}{\hbar} \frac{\partial E_{\min}(\varphi)}{\partial \varphi}, \quad (2)$$

where $\varphi = \varphi_L - \varphi_R$. However, note that the determination of the ground state is a formidable task, which requires some approximation scheme. A great simplification can be made by integrating out the electronic degrees of freedom of the superconducting leads. This procedure leads to an effective low energy theory in which each superconductor is replaced by a single site with an effective pairing potential $\tilde{\Delta}$. And, the hopping term $\tilde{V}_\alpha$ is replaced by an effective parameter $\tilde{V}_\alpha$. Accordingly, the new expressions of H_α and H_T are given by

$$H_\alpha = \sum_\sigma \varepsilon_\alpha a_{\alpha\sigma}^{\dagger} a_{\alpha\sigma} + \tilde{\Delta} e^{i\varphi_\alpha} a_{\alpha\downarrow} a_{\alpha\uparrow} + \tilde{\Delta} e^{-i\varphi_\alpha} a_{\alpha\uparrow}^{\dagger} a_{\alpha\downarrow}^{\dagger},$$
$$H_T = \sum_\sigma (\tilde{V}_L a_{L\sigma}^{\dagger} d_{1\sigma} + \tilde{V}_R a_{R\sigma}^{\dagger} d_{2\sigma} + \text{H.c.}). \quad (3)$$

This approach, usually referred to as the zero bandwidth model (ZBWM), has been discussed in some previous studies.[9,13,33] One can see that the ZBWM can give qualitatively correct results and can grasp the ground-state properties in this kind of system in the approximate range $\Gamma \leqslant \Delta$, where Γ is the standard tunneling rate to the leads. We should mention that the Hilbert space of the new system within the ZBWM is restricted to 4^5 states and the z component of the total spin S is a good quantum number. Thus, the eigenstates can be characterized in terms of S_z and the eigenenergies can be obtained by the block diagonalization of the Hamiltonian matrix.

III. NUMERICAL RESULTS AND DISCUSSIONS

Using the formulas developed above, we next calculate the Josephson current in the S/TQDR/S structure. For calculation, we consider that the temperature is zero and $\tilde{\Delta} = \tilde{V}_\alpha = 1$, i.e., all the energy quantities are scaled by $\tilde{\Delta}$. In principle, the effective parameters $\tilde{\Delta}$ and $\tilde{V}_\alpha$ in this approach have to be determined from the bare parameters Δ and V_α by means of a self-consistency condition and a renormalization-group analysis.[34] However, here we shall adopt the simplified assumption that $\tilde{\Delta} = \Delta$ and $\tilde{V}_\alpha = V_\alpha$ without an attempt to fine tune them within the range of parameters considered. This is a reasonable choice as far as we are interested in the qualitative trends rather than in the detailed quantitative results. In addition, we set the Fermi energy of the leads to be zero and consider $\varphi_L = -\varphi_R = \frac{\varphi}{2}$.

The Josephson current in the superconducting system with the embedded QDs is characterized by its phase. In order to completely analyze the Josephson current, we first demonstrate the phase of the Josephson current. Generally speaking, in such a structure four different ground states can be distinguished, i.e., the pure 0, π, 0′, and π' states. For the former two cases, the ground-state energy as a function of the superconducting phase difference $\varphi = \varphi_L - \varphi_R$ has a global minimum at the points of $\varphi = 0$ and $\varphi = \pi$, respectively. Alternatively, for the 0′ and π' phases, a local minimum is observed except the global minimum at the points of $\varphi = 0$ or $\varphi = \pi$.

Figure 1(a) shows a (ε_0, U) phase diagram for the 0-π transition of the Josephson current. The inter-dot coupling is taken to be $t_0 = 2.0$. In this figure, one can see that the intradot Coulomb interaction makes a leading contribution to the occurrence of the phase transition. In the weak Coulomb interaction case (e.g., $U \leqslant 5$), two phase-transition regions appear in the vicinity of $\varepsilon_0 = 0$ and $\varepsilon_0 \approx -U - 4$. To be concrete, in the region of $\varepsilon_0 \approx -U - 4$, the $0 \to 0'$ phase transition is only observed, whereas in the other region the phase transition $0 \to \pi \to \pi' \to 0'$ happens with the shift of the QD level. Next, with the strengthening of the Coulomb

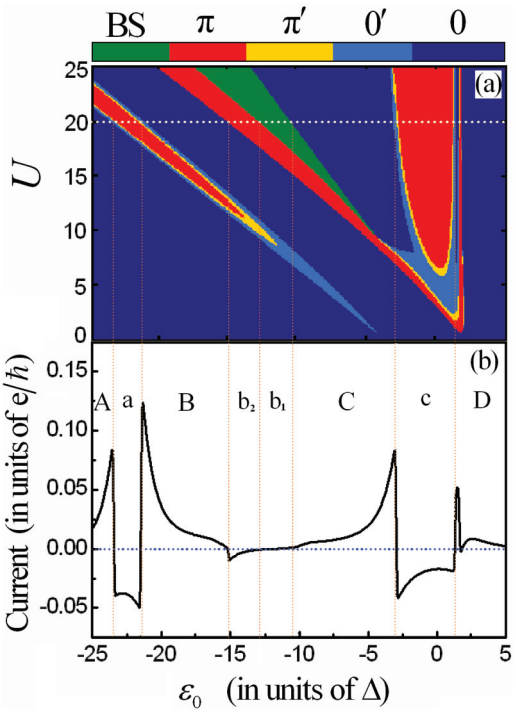

FIG. 1. (Color online) (a) The phase diagram of the Josephson current of the S/TQDR/S structure in the ZBWM. (b) The Josephson current as a function of QD level ε_0 with $U = 20$. The other parameters are taken to be $t_0 = 2.0$ and $\varphi = \frac{\pi}{2}$.

interaction, the phase-transition region in the vicinity of $\varepsilon_0 = 0$ splits. Then in the phase diagram, three 0-π transition regions respectively appear in the vicinity of $\varepsilon_0 = 0$, $\varepsilon_0 \approx -U - 4$, and $\varepsilon_0 \approx -\frac{U}{2}$. In the *left* ($\varepsilon_0 \approx -U - 4$) and *right* ($\varepsilon_0 = 0$) 0-$\pi$ transition regions, the phases 0, 0′, π', and π arise successively with the change of ε_0. But for the *central* one (where $\varepsilon_0 \approx -\frac{U}{2}$), the 0′ and π' phases disappear with the increase of U. Instead, when $U \geqslant 10$ a phase marked by *BS* is observed, and the *BS* phase region is gradually widened by the increase of Coulomb strength. In addition, we see that in such a *BS*-phase region, the phase-transition process is asymmetric about the change of QD level. For instance, in the case of $U = 20$, when the QD level decreases from $\varepsilon_0 = -9.0$ to $\varepsilon_0 = -15.0$ the Josephson current undergoes the 0, *BS*, π, and 0 phases, respectively. Therefore, in this structure the intradot Coulomb interaction contributes to a phase transition of the Josephson current.

The appearance of the *BS* phase is certain to change the properties of the Josephson current. With this idea, in Fig. 1(b) we focus on the case of $U = 20$ and plot the Josephson current as a function of ε_0. Here the superconducting phase difference is taken to be $\varphi = \frac{\pi}{2}$. It is obvious that the Josephson current oscillates seriously with the change of ε_0, and the properties of the Josephson current exactly correspond to the phase transition.[35] Concretely, I_J is positive in the corresponding 0-phase regions marked by *A*, *B*, *C*, and *D*. In the π-phase regions (marked by *a*, b_2, and *c*) I_J becomes less than zero. The reversal of the Josephson current direction corresponds to the phase transition. In region b_1, however, the Josephson current is almost equal to zero, independent of the change of the QD level. Based on these results, the relation between the *BS* phase and the Josephson current has been clarified.

In Eq. (2), one can notice that the phase transition of the Josephson current is determined by the ground-state energy of this system. So, in Fig. 2 we present the curves of the ground-state and the first excited state energies of the system affected by the superconducting phase difference φ. Here, we only focus on the left and central 0-π transition regions because the mechanism of the right one is similar to that of the former one. Figures 2(a)–2(d) correspond to the phase-transition process in the left phase-transition region in Fig. 1(a), where the $0 \to 0' \to \pi' \to \pi$ quantum phase transition occurs with the change of ε_0. Here we can find that the zero-value Josephson current (green dashed lines) in Figs. 2(a) and 2(d) appear at the points of $\varphi = 0$ and $\varphi = \pi$, respectively. Thus, the direction of the Josephson current is changed. For the results in Figs. 2(b) and 2(c), the energy levels of the ground (blue solid line) and the first excited states (red dashed-dotted lines) are crossed and the currents show a kinklike result, so the intermediate phases 0′ and π' come into being. This phenomenon is attributed to the competition between the Kondo effect and superconductivity.

For the phase transition in the central region in Fig. 1(a), we can analyze it with the help of Figs. 2(e)–2(h). In this figure, we can see that the intermediate phase is not the result of the crossing of the different energy levels, and that no kink is found in the current curves. Instead, in the intermediate phase, the curve of the ground-state energy has two global minima in one period of φ, which are symmetric about the point of $\varphi = \pi$. We thus call this state a *BS*-phase state. Based on this

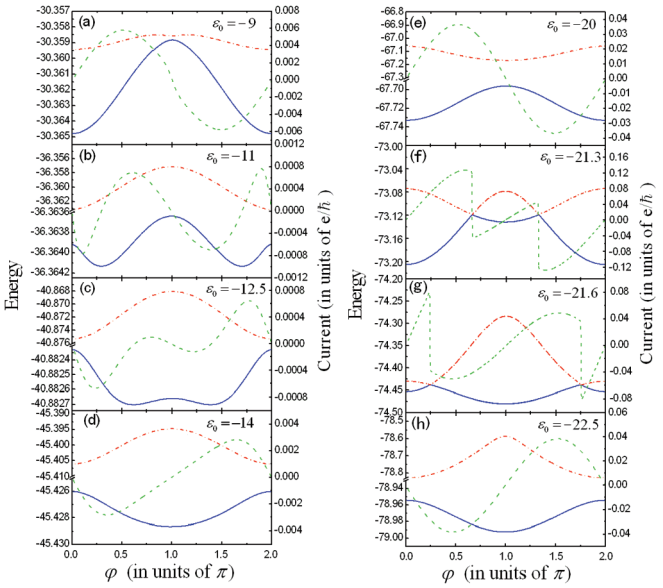

FIG. 2. (Color online) The ground-state energy levels and Josephson current as functions of the superconducting phase difference φ. The solid (blue), dashed-dotted (red), and dashed (green) lines correspond to the ground states, first excited states, and Josephson currents, respectively. The other parameters are taken to be $t_0 = 2.0$ and $U = 20$.

result, we can understand the appearance of the *BS* phase. In the 0-π phase-transition process, with the decrease of ε_0, the magnitude of the central peak in the curve of the ground-state energy will decrease until such a peak becomes a minimum. In such a process, if no energy-level crossing occurs, two minima inevitably emerge in one period of φ.

We next analyze the electron correlation in this structure to clarify the appearance of the *BS* phase. Figure 3 shows the average electron occupation and the interdot and dot-lead spin correlation as functions of ε_0. From Fig. 3(a), we observe that the opposite-spin electrons occupy the QDs with the equal opportunity in regions *A*, *B*, and *D*. Accordingly, the system is in an $S = 0$ ground state in these regions, which just leads to the appearance of the 0 phase. In region *a* and region *c*, we find the results that $S = \frac{1}{2}$ and $S = 1$, respectively. Previous research

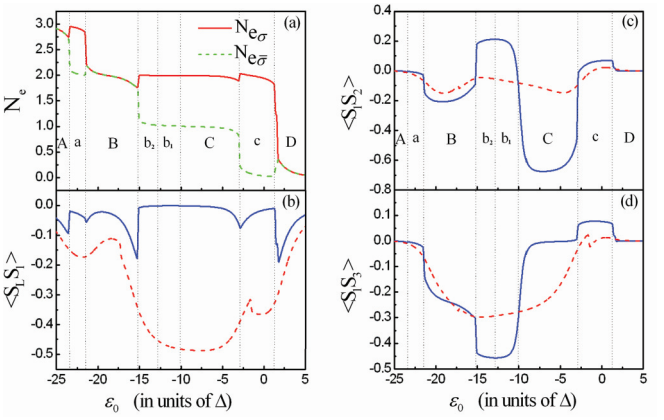

FIG. 3. (Color online) (a) The average electron occupation number in the TQDR. (b) The electron correlation between QD-1 and lead-*L*. (c),(d) The electron correlation between QDs.

demonstrated that in two such regions the $S = \frac{1}{2}$ and $S = 1$ Kondo effects will occur.[30,36] As a result, the interplay between the Kondo effect and superconductivity induces the π phase of the Josephson current. What is interesting is that in regions b_2, b_1, and C, the result of $S = \frac{1}{2}$ is robust, but the Josephson current is manifested as the π, BS, and 0 phases, respectively. This means that in these three regions the spin-correlation properties become complicated, as shown in Figs. 3(b)–3(d). In these figures, we can observe that in the three regions, the value of $\langle S_L S_1 \rangle$ remains equal to zero. This exactly indicates that the Kondo effect is suppressed. For the interdot spin correlations, however, they exhibit different results. In region b_2, $\langle S_1 S_2 \rangle = 0.2$ and $\langle S_1 S_3 \rangle = -0.45$. Hence in such a case, the electrons in QD-1 and QD-2 exhibit the ferromagnetic correlation, whereas the antiferromagnetic correlation occurs between QD-1(2) and QD-3. According to this result, we illustrate the Cooper pair tunneling in Figs. 4(a)–4(c). It is clearly seen that such electron correlation results in the high-order electron motion in the down arm of the TQDR; accordingly, the π phase comes into being. On the other hand, with respect to the spin correlation in region C, we find in Fig. 3 that $\langle S_1 S_2 \rangle = -0.7$ and $\langle S_1 S_3 \rangle = 0.0$. Thus, different from the results in region b_2, the antiferromagnetic correlation occurs between QD-1 and QD-2 in region C. It is certain that herein the spin state in QD-3 decouples from the singlet state formed by QD-1 and QD-2. Such a correlation mechanism exactly induces the other electron motion picture shown in Figs. 4(d)–4(f). To be specific, the electron motion is mainly driven by the correlation in the upper arm of this TQDR, so the 0 phase of I_J arises. Up to now, we have known that the π and 0 phases of the Josephson current in regions b_2 and C are driven by the unique mechanisms of the interdot spin correlations, respectively.

When the QD level shifts from $\varepsilon_0 = -9.0$ to $\varepsilon_0 = -12.0$, the electron correlations $\langle S_1 S_2 \rangle$ and $\langle S_1 S_3 \rangle$ change continuously [see Figs. 3(c) and 3(d)]. Thus, in such a regime,

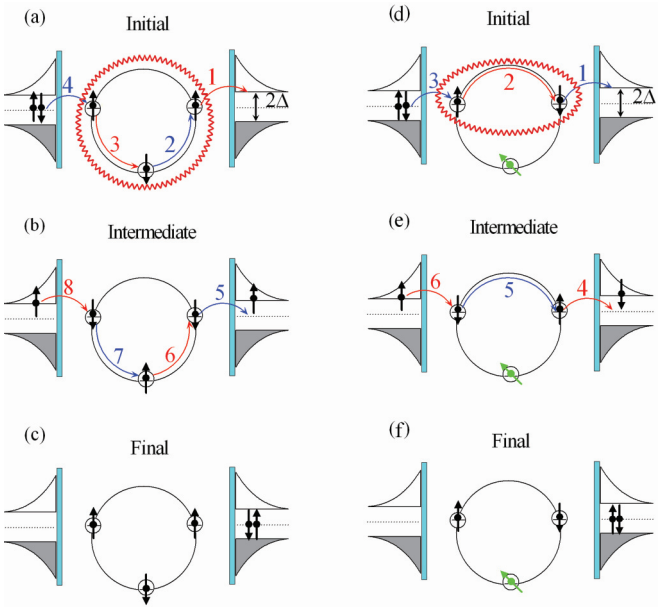

FIG. 4. (Color online) (a)–(c) The illustration of electron motion in region b_2. (d)–(f) The illustration of electron motion in region C.

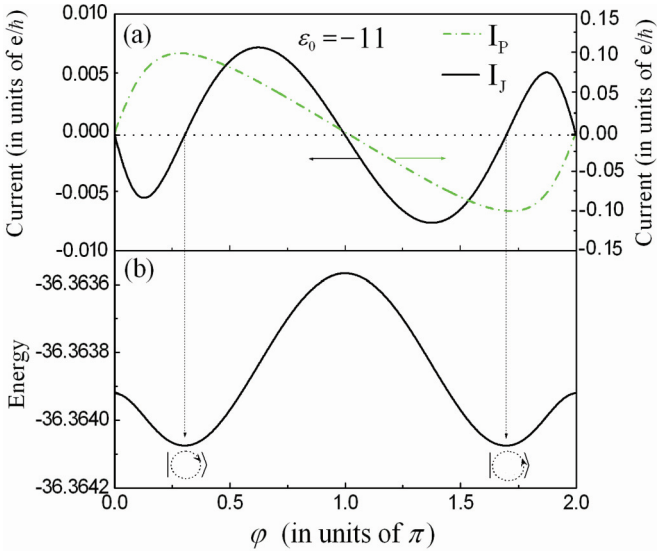

FIG. 5. (Color online) (a) The Josephson and persistent currents in the case of $\varepsilon_0 = -11.0$. (b) The ground-state energy tuned by the superconducting phase difference φ.

the two kinds of electron motion in Figs. 4(a)–4(c) and 4(d)–4(f) will coexist. Consequently, the electron motion in Figs. 4(d)–4(f), which mainly occurs in the upper arm of the TQDR, induces the 0-phase Josephson current. But the electron motion shown in Figs. 4(a)–4(c), contributed by the down arm, tends to cause the π-phase Josephson current. The 0-phase and π-phase Josephson currents are opposite, therefore, the coexistence of these two different electron motions certainly leads to the disappearance of the Josephson current through this structure. On the other hand, we notice that in comparison with the electron motion in Figs. 4(d)–4(f), in Figs. 4(a)–4(c) the electron motion can be considered to be resonant, because electrons will visit QD-3 in such a case. It therefore clear that when the "resonant" and "nonresonant" electron motion coexist, the interdot spin correlation will drive the zero Josephson current. As is known, the co-occurrence of the nonresonant and resonant electron tunneling results in the Fano effect. Accordingly, in such a case, the disappearance of the Josephson current can be called the Josephson-Fano effect. With the help of the above analysis, the quantum transport properties in such a structure have therefore been clarified.

Since the considered structure is a quantum ring, we would like to study the persistent current in it. As is known, for an isolated ring, the persistent current can only be driven by a local magnetic flux. Its magnitude can be investigated by evaluating the interdot current between the jth and the $(j+1)$th QDs, i.e., $I_{j,j+1} = \frac{ie}{\hbar} \sum_\sigma \langle 0 | t_j d^\dagger_{j+1\sigma} d_{j\sigma} - \text{H.c.} | 0 \rangle$, where $|0\rangle$ denotes the ground state of the system. However, for our model with two leads, the quantum ring is open. It has been reported that in an open mesoscopic ring, the persistent current is not necessarily driven by a local magnetic flux through the ring. Benjamin and Jayannavar found that the persistent current can be observed at nonequilibrium with zero magnetic flux.[37] Namely, the persistent current in the open ring can be driven by the transport current through the ring. Accordingly, in a quantum ring with two leads, the persistent current can be

redefined as[35]

$$I_p = \begin{cases} 0, I_U \cdot I_L \leqslant 0 \\ [1-\theta(|I_U|-|I_L|)]\cdot I_U + \theta(|I_U|-|I_L|)\cdot I_L, \\ I_U \cdot I_L > 0. \end{cases} \quad (4)$$

$\theta(x)$ is the step function. I_U and I_L are the currents through the upper and lower arms, respectively. They are defined as $I_U = \frac{ie}{\hbar}\sum_\sigma \langle 0|t_1 d^\dagger_{2\sigma} d_{1\sigma} - \text{H.c.}|0\rangle$ and $I_L = \frac{ie}{\hbar}\sum_\sigma \langle 0|t_1 d^\dagger_{1\sigma} d_{3\sigma} - \text{H.c.}|0\rangle$. In Fig. 5(a), we present the persistent current and the Josephson current affected by the change of the superconducting phase difference between the leads. We only pay attention to the case where the phase of the Josephon current is the *BS* phase, since we would like to clarify the effect of the new phase on the persistent current. Without loss of generality, we choose $\varepsilon_0 = -11.0$. It can be found that in such a phase, the superconducting phase difference can drive finite persistent current in the ring. Similar to the Josephson current, the direction of the persistent current in the ring can also be adjusted by the change of φ. In the case of $\varphi = \frac{n}{2}\pi$ (n is integer), both the Josephson current and the persistent current are approximately equal to each other. And, if n is even, the two currents are completely suppressed. What is interesting is that when I_p reaches its extremum around the points of $\varphi = 0.3\pi$ and $\varphi = 1.7\pi$, the Josephson current disappears. And, at these two points the directions of the persistent current are opposite to each other. This means that in the *BS*-phase case, the superconducting phase difference can drive an isolated persistent current in the ring, accompanied by the "decoupling" of the leads from the TQDR. With the help of Fig. 5(b), we see that the maximal persistent current exactly corresponds to the minimum of the ground-state energy of this system. According to our above analysis, the appearance of the isolated persistent current can be well understood. In the *BS*-phase region, the two arms of the ring carry the opposite-direction currents. With the shift of QD level, one has a chance to get the result that $I_U = I_L$, hence the persistent current reaches its maximum accompanied by the disappearance of the Josephson current. Based on the results here, we consider such a structure to be a candidate for the persistent current bit.

Finally, we intend to discuss the role of the inter-dot coupling in achieving the appearance of the *BS* phase of the Josephson current. The numerical result is shown in Fig. 6. In this figure, it can clearly be found that the value of t_0 is a key factor to induce the Josephson phase transition. In the case of the weak interdot coupling, i.e., $t_0 < 1.7$, the Josephson current exhibits as a modified 0 phase, since the Josephson current is almost independent of the variation of φ near the region of $\varphi = \pi$. With the increase of t_0, such a current plateau is squeezed until its disappearance. As a result, around the position of $t_0 = 2.0$, the Josephson current shows three peaks and two valleys [see Fig. 2(g)], which just corresponds to the *BS*-phase case. The further increase of t_0 induces the appearance of the π-phase Josephson current. Next, in the case of $t_0 \geqslant 4.0$, the 0-phase Josephson current occurs again. With this result, we can clarify the role t_0 in adjusting the Josephson current. It is noteworthy that only when the interdot coupling is adjusted to be $t_0 \approx 2.0$, the Josepshon-Fano effect has an opportunity to come into being. In addition, by comparing the

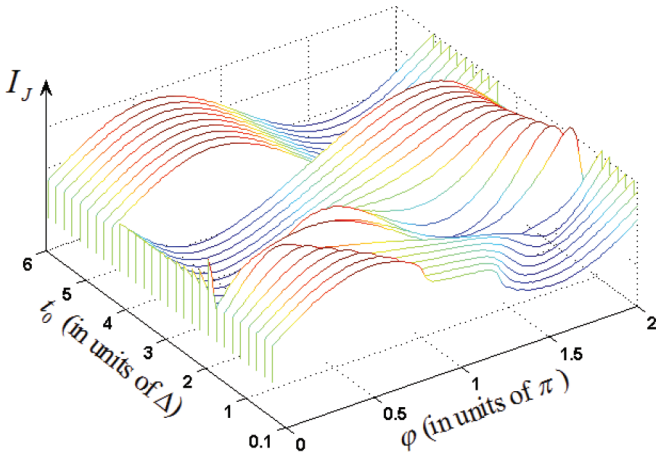

FIG. 6. (Color online) (a) The Josephson current with the change of t_0. The other parameters are the same as Fig. 2(g).

results in Fig. 6 and the central region of Fig. 1, we can find that the increase of t_0 plays a similar role as the decrease of ε_0 in inducing the phase transition. The main reason is that these two manipulations decrease the ground-state energy of such a structure in a similar way. Thus, the phase-transition results are almost the same.

IV. SUMMARY

In summary, we have investigated the Josephson effect in an S/TQDR/S structure by means of ZBWM. It has been found that two interdot spin-correlation mechanisms exist which cause the new 0 and π phases of the Josephson current. Moreover, in the 0-π phase-transition process, an intermediate *BS* phase appears in which the Josephson current is completely suppressed. By analyzing the interdot spin correlation, the electron motion mechanism has been clarified. We attributed the disappearance of the Josephson current to the occurrence of the Josephson-Fano effect. The interesting result is that the zero Josephson current is accompanied by the apparent persistent current in the ring whose direction is determined by the superconducting phase difference. With the results, we consider such a structure to be a candidate for the realization of the persistent current bit.

Finally, we would like to remark on the phase transition of the Josephson current in this structure. In such a structure, it is the alternate occurrence of the two interdot spin correlation [i.e., the correlations between QD-1 and QD-2 (or QD-3)] controlled by the shift of QD levels that modifies the quantum interference of the high-order electron motion. As a result, in the presence of appropriate structure parameters, the Josephson-Fano effect is induced. Therefore, the TQDR form of the structure is important for the Josephson phase transition. Alternatively, if the QD structure is changed, a similar phenomenon cannot arise. The reason is that the interdot spin correlation does not necessarily drive the resonant and nonresonant tunneling processes simultaneously. For instance of the T-shaped double QDs and the four-QD ring structures,[35,38] no *BS* phase was observed in spite of the interesting quantum transport properties in them.

ACKNOWLEDGMENTS

Our numerical results are obtained via an exact diagonalization program based on the SNEG library. This work was financially supported by Fundamental Research Funds for the Central Universities (Grants No. N100305002 and No. N110405010), the National Natural Science Foundation of China (Grant No. 10904010), and the Liaoning BaiQianWan Talents Program (Grant No. 2012921078). W.J.G. thanks Shu-Feng Zhang for his helpful discussion.

*gwjneu@163.com

[1] D. Goldhaber-Gordon, Hadas Shtrikman, D. Mahalu, David Abusch-Magder, U. Meirav, and M. A. Kastner, Nature (London) **391**, 156 (1998); S. M. Cronenwett, T. H. Oosterkamp, and L. P. Kouwenhoven, Science **281**, 540 (1998).

[2] M. R. Buitelaar, A. Bachtold, T. Nussbaumer, M. Iqbal, and C. Schonenberger, Phys. Rev. Lett. **88**, 156801 (2002); K. Grove-Rasmussen, H. I. Jorgensen, and P. E. Lindelof, New J. Phys. **9**, 124 (2007).

[3] J. Park, A. Pasupathy, J. I. Goldsmith, C. Chang, Y. Yaish, J. R. Petta, M. Rinkoski, J. P. Sethna, H. D. Abruna, P. L. McEuen, and D. C. Ralph, Nature (London) **417**, 722 (2002).

[4] P. Vitushinsky, A. A. Clerk, and K. LeHur, Phys. Rev. Lett. **100**, 036603 (2008); R. López, T. Rejec, J. Martinek, and R. Žitko, Phys. Rev. B **87**, 035135 (2013).

[5] S. Sasaki, H. Tamura, T. Akazaki, and T. Fujisawa, Phys. Rev. Lett. **103**, 266806 (2009).

[6] L. I. Glazman and K. A. Matveev, JETP Lett. **49**, 659 (1989) [Pis'ma Zh. Eksp. Teor. Fiz. **49**, 570 (1989)].

[7] A. V. Rozhkov and D. P. Arovas, Phys. Rev. Lett. **82**, 2788 (1999).

[8] A. A. Clerk and V. Ambegaokar, Phys. Rev. B **61**, 9109 (2000).

[9] E. Vecino, A. Martín-Rodero, and A. Levy Yeyati, Phys. Rev. B **68**, 035105 (2003).

[10] F. Siano and R. Egger, Phys. Rev. Lett. **93**, 047002 (2004).

[11] M. S. Choi, M. Lee, K. Kang, and W. Belzig, Phys. Rev. B **70**, 020502(R) (2004).

[12] G. Sellier, T. Kopp, J. Kroha, and Y. S. Barash, Phys. Rev. B **72**, 174502 (2005).

[13] F. S. Bergeret, A. Levy Yeyati, and A. Martín-Rodero, Phys. Rev. B **74**, 132505 (2006).

[14] Y. Tanaka, A. Oguri, and A. C. Hewson, New J. Phys. **9**, 115 (2007).

[15] B. I. Spivak and S. A. Kivelson, Phys. Rev. B **43**, 3740 (1991).

[16] J. A. van Dam, Yu. V. Nazarov, E. P. A. M. Bakkers, S. De Franceschi, and L. P. Kouwenhoven, Nature (London) **442**, 667 (2006).

[17] J.-P. Cleuziou, W. Wernsdorfer, V. Bouchiat, T. Ondarcuhu, and M. Monthioux, Nat. Nanotechnol. **1**, 53 (2006).

[18] H. Pan, R. Lu, and C. Wang, Solid State Commun. **144**, 37 (2007).

[19] H. Pan, L. Zhao, T. Lin, and D. Yu, Phys. Lett. A **367**, 237 (2007).

[20] L. Bai, Q. Zhang, L. Jiang, Z. Zhang, and R. Shen, Phys. Lett. A **374**, 2584 (2010).

[21] S. Amaha, T. Hatano, T. Kubo, Y. Tokura, D. G. Austing, and S. Tarucha, Physica E **40**, 1322 (2008); M. C. Rogge and R. J. Haug, Phys. Rev. B **77**, 193306 (2008).

[22] A. K. Mitchell, T. F. Jarrold, and D. E. Logan, Phys. Rev. B **79**, 085124 (2009); L. Gaudreau, S. A. Studenikin, A. S. Sachrajda, P. Zawadzki, A. Kam, J. Lapointe, M. Korkusinski, and P. Hawrylak, Phys. Rev. Lett. **97**, 036807 (2006); G. Granger, L. Gaudreau, A. Kam, M. Pioro-Ladrière, S. A. Studenikin, Z. R. Wasilewski, P. Zawadzki, and A. S. Sachrajda, Phys. Rev. B **82**, 075304 (2010).

[23] D. Loss and D. P. DiVincenzo, Phys. Rev. A **57**, 120 (1998).

[24] Y. Nagaoka, Phys. Rev. **147**, 392 (1966).

[25] A. D. Greentree, J. H. Cole, A. R. Hamilton, and L. C. L. Hollenberg, Phys. Rev. B **70**, 235317 (2004).

[26] M. Stopa, Phys. Rev. Lett. **88**, 146802 (2002).

[27] K. Ingersent, A. W. W. Ludwig, and I. Affleck, Phys. Rev. Lett. **95**, 257204 (2005).

[28] T. Kuzmenko, K. Kikoin, and Y. Avishai, Phys. Rev. Lett. **96**, 046601 (2006).

[29] R. Zitko, J. Bonča, A. Ramšak, and T. Rejec, Phys. Rev. B **73**, 153307 (2006).

[30] T. Numata, Y. Nisikawa, A. Oguri, and A. C. Hewson, Phys. Rev. B **80**, 155330 (2009).

[31] M. Seo, H. K. Choi, S.-Y. Lee, N. Kim, Y. Chung, H.-S. Sim, V. Umansky, and D. Mahalu, Phys. Rev. Lett. **110**, 046803 (2013).

[32] W. Gong, Y. Zheng, and T. Lü, Appl. Phys. Lett. **92**, 042104 (2008).

[33] F. S. Bergeret, A. Levy Yeyati, and A. Martín-Rodero, Phys. Rev. B **76**, 174510 (2007).

[34] I. Affleck, J.-S. Caux, and A. M. Zagoskin, Phys. Rev. B **62**, 1433 (2000).

[35] G. Yi, L. An, W.-J. Gong, H. Wu, and G. Wei, J. Appl. Phys. **112**, 033717 (2012).

[36] A. Oguri, S. Amaha, Y. Nishikawa, T. Numata, M. Shimamoto, A. C. Hewson, and S. Tarucha, Phys. Rev. B **83**, 205304 (2011).

[37] C. Benjamin and A. M. Jayannavar, Phys. Rev. B **64**, 233406 (2001).

[38] G. Yi, L. An, W.-J. Gong, H. Wua, and X. Chen, Phys. Lett. A **377**, 1127 (2013).